Diarylheptanoids from *Alnus japonica* Inhibit Papain-Like Protease of Severe Acute Respiratory Syndrome Coronavirus

Ji-Young Park,[a,b] Hyung Jae Jeong,[a] Jang Hoon Kim,[a] Young Min Kim,[a] Su-Jin Park,[a] Doman Kim,[b] Ki Hun Park,[c] Woo Song Lee,*[,a] and Young Bae Ryu*[,a]

[a] *Infection Control Material Research Center, Korea Research Institute of Bioscience and Biotechnology (KRIBB); Jeongeup 580–185, Republic of Korea:* [b] *School of Biological Science and Biotechnology, Chonnam National University; Gwangju 500–757, Republic of Korea: and* [c] *Division of Applied Life Science (BK 21 Program, IALS), Graduate School of Gyeongsang National University; Jinju 660–701, Republic of Korea.*

The papain-like protease (PL^{pro}), which controls replication of the severe acute respiratory syndrome coronavirus (SARS-CoV), has been identified as a potential drug target for the treatment of SARS. An intensive hunt for effective anti-SARS drugs has been undertaken by screening for natural product inhibitors that target SARS-CoV PL^{pro}. In this study, diarylheptanoids 1–9 were isolated from *Alnus japonica*, and the inhibitory activities of these compounds against PL^{pro} were determined. Of the isolated diarylheptanoids, hirsutenone (2) showed the most potent PL^{pro} inhibitory activity, with an inhibitory concentration (IC$_{50}$) value of 4.1 μM. Structure–activity analysis showed that catechol and α,β-unsaturated carbonyl moiety in the molecule were the key requirement for SARS-CoV cysteine protease inhibition.

Key words diarylheptanoid; *Alnus japonica*; severe acute respiratory syndrome; papain-like protease; cysteine protease

Severe acute respiratory syndrome (SARS), a contagious and often fatal respiratory illness, was first reported in Guandong province, China, in November 2002. Its rapid and unexpected spread to other Asian countries, North America, and Europe alarmed both the public and the World Health Organization (WHO). SARS is a life-threatening form atypical pneumonia caused by infection with a novel human coronavirus (SARS-CoV).[1–3] SARS-CoV is a plus-strand RNA virus that encodes four structural proteins, 16 nonstructural proteins, and 8 accessory proteins.[2,4] The 16 nonstructural proteins are the cleavage products of the 2 large polypeptides pp1a and pp1ab and are generated by the virally encodes proteases 3-chymotrypsin-like protease (3CL^{pro}) and papain-like protease (PL^{pro}, EC 3.4.22.46).[5–8] These proteases are considered the most prominent and effective drug targets in antiviral therapies. Because proteolytic processing is essential for the generation of a functional replication complex, 3CL^{pro} and PL^{pro} are potentially effective targets for anti-SARS drugs. Most efforts reported to date have focused on the development of 3CL^{pro} inhibitors, which have been identified in both synthetic peptidyl libraries[9–11] and natural derived libraries.[12,13] Fewer inhibitors of PL^{pro} have been studied, and those that have been studied include thiopurine analogs and benzamide derivatives.[14,15] No naturally derived inhibitor of this protease has been reported previously. In the study described in this letter, an intensive hunt for effective anti-SARS drug was undertaken by screening natural products for inhibitory activity against SARS-CoV PL^{pro}.

Natural products have been found to be an important source of drug and drug leads. As part of our screening of SARS-CoV PL^{pro} inhibitors from natural sources, we found that an ethanol extract of the stem bark of *Alnus japonica* exhibited PL^{pro} inhibitory activity. *Alnus japonica* (Betulaceae) has led to the identification of numerous diarylheptanoids. Diarylheptanoids, such as curcumin, belong to a phenolic class of natural products based on 1,7-diphenylheptane skeleton. *Alnus japonica* and its constituents exhibit various biological properties, including anti-inflammatory, anticancer, and anti-influenza activities.[16–18] To the best of our knowledge, the study of this plant with respect to SARS-CoV papain-like cysteine protease inhibition has never been reported. In this study, we expressed and purified in *Escherichia coli* (*E. coli*) the full length PL^{pro} as well as truncated forms containing only the catalytic domains.

MATERIALS AND METHODS

General ^{1}H- and ^{13}C-NMR along with 2D-NMR data were obtained on JNM-EX 400 (Jeol, Japan) spectrometers in methaol-d_6 and tetramethylsilane (TMS) as internal standards. Electrospray ionization (ESI) mass spectra were scanned using ESI in negative or positive mode with bruker esquire 6000 mass spectrometer. All of the reagent grade chemicals were purchased from Sigma-Aldrich Chemical Co. (St. Louis, MO, U.S.A.). Chromatographic separations were carried out by thin-layer chromatography (TLC) (E. Merck Co., Darmastdt, Germany), using commercially available glass plates precoated with silica gel and visualized under UV at 254 and 366 nm. Column chromatography was carried out using 230–400 mesh silicagel (Kieselgel 60, Merck, Germany). RP-18 (ODS-A, 12 μm, S-150 Å, YMC) and Sephadex LH-20 (Amersham Biosciences) were used for column chromatography.

Plant Material and Preparation of Extracts The air-dried bark of *Alnus japonica* (3.0 kg) was extracted with 95% ethanol (2×10 L) at room temperature for a week. The combined extract was concentrated *in vacuo* to give a dark residue (122 g). The crude extract was suspended in water and successively partitioned with organic solvents (hexane and ethyl acetate) of the different polarities to obtain fractions of hexane (13 g), ethyl acetate (36 g) and H$_2$O (69 g). The ethyl acetate fraction (36 g) was fractionated over a silica gel
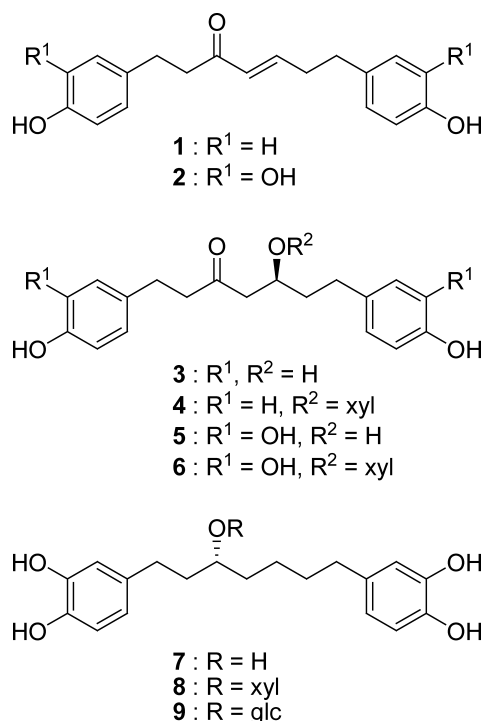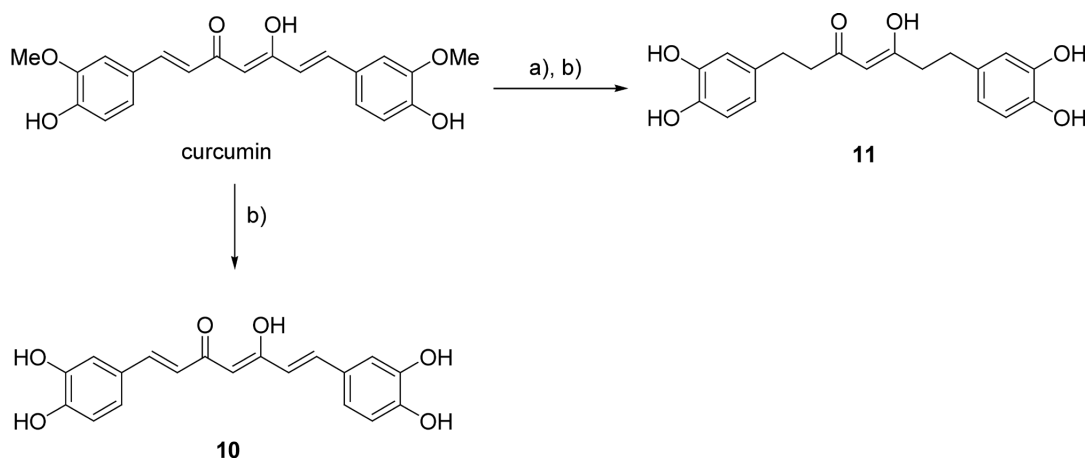
Fig. 1. Chemical Structures of Isolated Diarylheptanoids from *A. japonica* (xyl: *β*-D-Xylopyranosyl and glc: *β*-D-Glucopyranosyl)

column (10×30 cm, 230–400 mesh; Merk) using a gradient of chloroform–acetone (30:1→1:1, v/v) to yield nine fractions (fr. 1–fr. 9) based on TLC profile. Fraction 6 (1.0 g) was chromatographed over a Sephadex LH-20 column (2×90 cm) using MeOH as eluting solvent to give four fractions (fr. 61–fr. 64); fr. 62 and fr. 63 (235.7 mg) was resubjected to RP-18 (ODS-A, 12 nm, S-150 mM, YMC) chromatography to yield give compound **6** (200 mg). The fraction 7 (7.2 g) was separated through chromatography on Sephadex LH-20 column (mobile phase: MeOH), a RP-C18 chromatography column and preparative-HPLC to yield compounds **1** (27 mg), **3** (49 mg) and compound **4** (54 mg). Next, compounds **7** (8 mg) and **8** (38 mg) were isolated from fraction 5 (1.6 g) using a Sephadex LH-20 column and a RP-C18 chromatography column.

Fraction 3 (1.6 g) was chromatographed by Sephadex LH-20 to give five fractions (fr. 31–35). Fraction 32 was subjected to RP-C18 chromatography column chromatography (mobile phase: 85% acetonitile) yielding five fractions (fr. 321–325). Fractions 321–323 were identical to compound **2** (350 mg). Finally, fraction 8 (1 g) was purified *via* Sephadex LH20 column chromatography (mobile phase: MeOH) to give six fractions (fr. 81–86). Then, 62 mg of compound **9** were gained from fr. 84. The physical and spectroscopic data of compounds **1–9** agree with those previously published[14,16)] for platyphyllenone (**1**), hirsutenone (**2**), platyphyllone (**3**), platyphyllonol-5-xylopyranoside (**4**), hirsutanonol (**5**), oregonin (**6**), rubranol (**7**), rubranoside B (**8**) and rubranoside A (**9**) (Fig. 1).

Synthesis of Compounds 10 and 11 The keto-enol derivatives (**10**, **11**) were synthesized from curcumin, as shown in Chart 1. A solution of curcumin (200 mg, 0.54 mmol) in dry CH_2Cl_2 (30 mL) was stirred at −50°C for 10 min and BBr_3 (2.5 mL, 17% in CH_2Cl_2) was slowly added. On completion of the reaction, water was added and the mixture was extracted with EtOAc. The combined organic phase was washed with H_2O, dried over anhydrous $MgSO_4$. The solvent was evaporated, and then the crude product was subjected to purification through silica gel column chromatography (*n*-hexane : ethyl acetate=1 : 1) to afford **10** in 20% yields. For selective reduction of *α,β*-carbonyl group in curcumin, platinum on activated charcoal (25 mg, 10% Pt basis) was added methanol solution (50 mL) containing curcumin (1.0 g, 2.7 mmol) at room temperature and the reaction mixture was stirred at room temperature for 8 h at H_2 atmosphere. On completion of the reaction, the suspended material was removed by filtration and filtrate was evaporated, and then the crude product was subjected to purification through silica gel column chromatography (*n*-hexane : ethyl acetate=1 : 1) to afford tetrahydrocurcumin in 40% yields. Tetrahydrocurcumin was subjected to demethylation in similar manner to that of compound **10** to give compound **11** (25%).

Preparations of SARS-CoV 3CL^{pro} and PL^{pro} The two genes encoding the 3CL protease and PL protease of SARS-CoV were designed based on the sequence reported by Sun *et al.*[19)] and Han *et al.*[20)] The synthesized genes were inserted into protein expression vector so that 3CL^{pro} and PL^{pro} are tagged with 6× histidine at the C-terminus. Expression

Reagents and conditions: a) H_2/Pt-C, MeOH; b) BBr_3, CH_2Cl_2, −50°C.

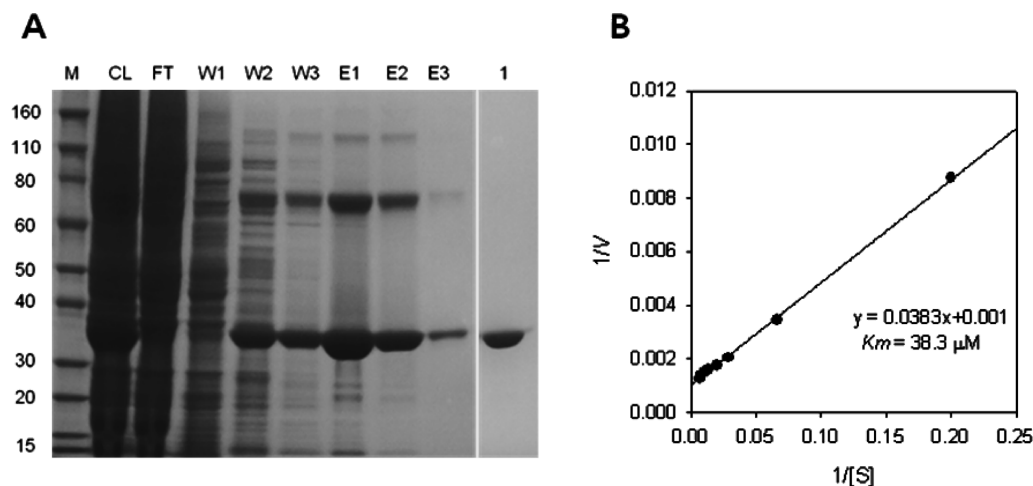Chart 1. Catalytic Hydrogenation and Demethylation of Curcumin

Fig. 2.   (A) Purification of SARS-CoV PL^{pro}; (B) Lineweaver–Burk Plot for the Determination of the PL^{pro} K_m Value

(A) M, protein molecular-weight markers (kDa); CL, cell lysate; FT, flow-through; W1, 20 mM imidazole wash; W2 and W3, 50 mM imidazole wash; E1, E2 and E3, 100–300-mM imidazole elution; 1, concentrated protein using an Amicon Ultra 10,000 MW cut-off. (B) The reaction was done at various substrate concentrations to obtain K_m value of the enzyme. SigmaPlot was used to fit the kinetic data using Lineweaver–Burk double reciprocal plots.

of recombinant 3CL^{pro} and PL^{pro} were induced with 0.5 mM isopropyl β-D-thiogalactopyranoside in *E. coli* BL21 (DE3) CodonPlus-RIL (Stratagene, La Jolla, CA, U.S.A.) during mid-log phase. The cells were grown at 16°C for 12 h, followed by sonication in buffer A (20 mM sodium phosphate, 300 mM NaCl, 10 mM imidazole, 0.2% Triton X-100, pH 7.5), and centrifuged at 15000×*g* for 30 min. The supernatant was loaded on a Ni-Sepharose column equilibrated with buffer A, and the recombinant protein was eluted by buffer A with 100–200 mM imidazole. The purified proteases ran approximately at the calculated size of 33 kDa (3CL^{pro}) and 36.5 kDa (PL^{pro}, Fig. 2A) on sodium dodecyl sulfate-polyacrylamide gel electrophoresis (SDS-PAGE). The elution buffer was then changed to 20 mM Tris–HCl buffer (pH 7.5) with 1 mM dithiothreitol, and the protein was concentrated using an Amicon Ultra filter with a 10000 molecular weight cut-off (Millipore, Billerica, MA, U.S.A.). The enzyme concentration was determined from its absorbance at 280 nm. To calculate the kinetic parameters of the purified 3CL^{pro} and PL^{pro}, enzyme activity was analyzed with fluorescent substrate from 1.25 to 100 μM. The K_m value were 32.0±5.2 μM (3CL^{pro}) and 38.3±1.8 μM (PL^{pro}, Fig. 2B). The purified proteins were stored at −80°C before use in any of the assays.

SARS-CoV 3CL^{pro} Inhibition Assay   As described,[21] the inhibitory effects of each compound on the enzymatic activities of 3CL^{pro} was evaluated using purified enzyme and fluorogenic substrate peptide. In this assay, the 12-mer fluorogenic peptide Dabcyl-KNSTLQSGLRKE-Edans (Anygen Co., Republic of Korea) was used as a substrate, and the enhanced fluorescence due to cleavage of this substrate catalyzed by the protease was measured at 590/40 nm with excitation 360 nm using a fluorescence plate reader (BioTeck Instrument Inc., U.S.A.). The inhibitory concentration (IC$_{50}$) values of isolated compounds were measured in a reaction mixture containing 10 μg/mL of the 3CL^{pro} (final concentration, 2.5 μg), the test compounds (from 0 to 200 μM), and 10 μM of fluorogenic 12-mer peptide substrate in 20 mM Bis-Tris buffer (pH 7.5). The reactions were run for 60 min at 37°C while continuously monitoring the fluorescence. The initial velocities of the inhibited reactions were plotted against the different concentrations

of inhibitor to obtain the IC$_{50}$ values by properly fitting the data according to the analysis method previously reported.[13]

SARS-CoV PL^{pro} Inhibition Assay   The PL^{pro} inhibition assay applied report by Ratia *et al.*[22] The inhibition assay was optimized in a 96-well plate format to establish suitable assay conditions and incubation times. The fluorogenic peptide substrate, Arg-Leu-Arg-Gly-Gly-AMC (RLRGG-AMC), was purchased from Bachem Bioscience. The enhanced fluorescence emission upon substrate cleavage was monitored at excitation and emission wavelengths of 360 and 460 nm, respectively, in a SpectraMax M^{2e} Multimode Reader (Molecular Devices Co., U.S.A.). The reaction mixture contained 54 nM PL^{pro} in 20 mM Tris–HCl buffer (pH 6.8) in a total volume of 200 μL. After the addition of 30 μM substrate to the reaction mixture, the increase in fluorescence at 460 nm was continuously monitored at 37°C. For the inhibition studies, 54 nM PL^{pro} and 0–200 μM of the individual compounds were mixed with the substrate (30 μM) at 37°C, and the fluorescence intensity was monitored. For the determination of enzyme activity (fitting experimental data to the logistic curve by (Eq. 1), used time-drive protocol with initial velocity was recorded over a range of concentrations and the data were analyzed using a nonlinear regression program [Sigma Plot 10.0 (SPCC Inc., Chicago, IL, U.S.A.)].

$$\text{Activity } (\%) = 100[1/(1+([I]/IC_{50}))] \qquad (1)$$

The inhibition mechanism was determined, and the apparent inhibition constants (K_i) for the respective PL^{pro} enzymes were performed on the test compounds, for which the IC$_{50}$ values were below 200 μM. In general, the test compounds were studied at three different concentrations that were chosen based on the IC$_{50}$ values obtained with each PL^{pro} enzyme (approximately 1/2×IC$_{50}$, IC$_{50}$, 2×IC$_{50}$). The concentrations of marker substrates were chosen (approximately 1/4 K_m, 1/2 K_m, K_m) with regard to their Michaelis–Menten kinetics (K_m and V_{max}). The K_i values were calculated by nonlinear regression analysis by fitting different models of enzyme inhibition to the kinetic data using SigmaPlot Enzyme Kinetics Module 1.3 (SPSS Inc., Chicago, IL, U.S.A.). The inhibition mechanism of compounds were determined by comparing the statistical results including the Akaike's information criterion values of
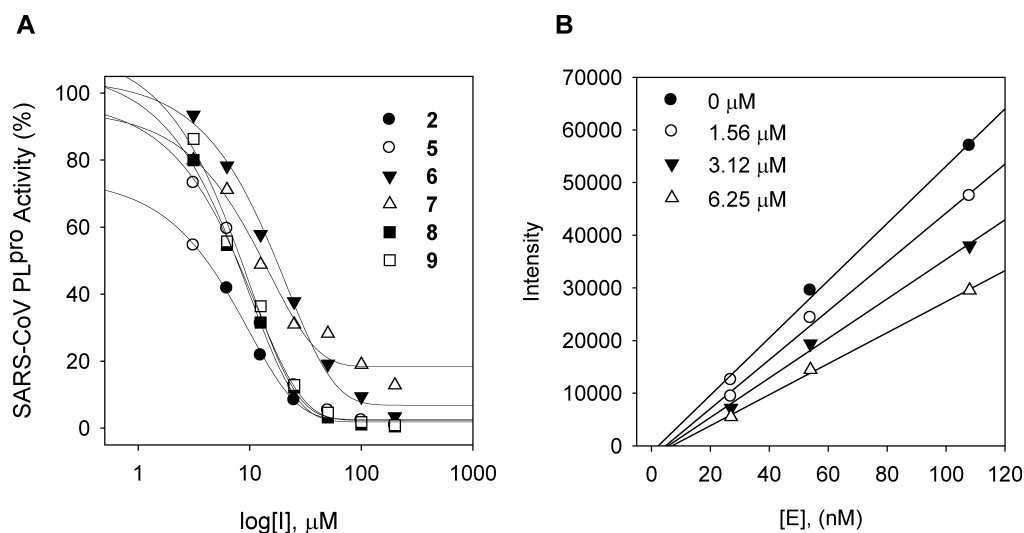
A **B**

Fig. 3. (A) Effects of Diarylheptanoids (**2**, **5**–**9**) in the Activity of SARS-CoV PL^{pro} and (B) Relationship of the Hydrolytic Activity of SARS-CoV PL^{pro} Concentrations at Different Concentrations of Compound **2**

Table 1. SARS-CoV PL^{pro} Inhibitory Activity of Diarylheptanoid Derivatives (**1**–**11**) and Curcumin

Compound	SARS-CoV PL^{pro}, IC$_{50}$ (μM)$^{a)}$	Inhibition type	K_m	K_i
1	>200	NT$^{b)}$	NT	NT
2	4.1±0.3	Noncompetitive	14.9±0.9	10.1±0.4
3	>200	NT	NT	NT
4	>200	NT	NT	NT
5	7.8±1.7	Mixed-type	16.8±2.7	13.2±3.6
6	20.1±2.2	Noncompetitive	9.8±6.7	21.5±3.5
7	12.3±0.9	Uncompetitive	20.2±2.0	9.2±0.6
8	8.0±0.2	Noncompetitive	18.6±3.3	18.0±1.9
9	9.1±1.0	Noncompetitive	23.2±4.6	39.3±0.4
10	6.2±2.2	NT	NT	NT
11	59.8±1.3	NT	NT	NT
Curcumin	5.7±0.3	NT	NT	NT

a) All compounds were examined in a set of experiments repeated three times; IC$_{50}$ values of compounds represent the concentration that caused 50% enzyme activity loss. *b*) Not tested.

different inhibition models and selecting the one with the best fit.[23)]

SARS-CoV PL^{pro} Deubiquitination Assay For the deubiquitination assay, purified PL^{pro} (54 nM) was mixed with fixed compound concentration of of 0–200 μM before the substrate, Ubiquitin-AMC (Enzo Life sciences Inc., U.S.A.), was added in 20 mM Tris–HCl buffer (pH 6.8). All assays were performed at 37°C in 96-well plate format. The enzyme activities were determined by monitoring the enhanced fluorescence emission upon substrate cleavage at excitation and emission wavelengths of 360 and 460 nm, respectively, in a SpectraMax M^{2e} Multimode Reader (Molecular Devices Co., U.S.A.). The substrate concentration was 100 nM, and release of AMC was measured in the same manner as for the IC$_{50}$ measurements described above.[22)]

RESULTS AND DISCUSSION

SARS-CoV PL^{pro} inhibitory activity-guided fractionation of the ethanol extract led to the isolation of nine diarylheptanoids (**1**–**9**) (Fig. 1). The isolated diarylheptanoids **1**–**9** were identified by spectroscopic data as platyphyllenone (**1**), hirsutenone

Table 2. SARS-CoV 3CL^{pro} and Ubiquitinase Inhibitory Activity of Isolated Diarylheptanoids (**1**–**9**)

Compound	SARS-CoV 3CL^{pro}, IC$_{50}$ (μM)$^{a)}$	Deubiquitination activity, IC$_{50}$ (μM)
1	>200	>200
2	36.2±2.0	3.0±1.1
3	>200	>200
4	>200	>200
5	105.6±6.5	24.1±2.0
6	129.5±3.1	44.5±5.3
7	144.6±4.8	35.2±1.7
8	105.3±1.7	7.2±2.2
9	102.1±2.5	14.4±3.0

a) All compounds were examined in a set of experiments repeated three times; IC$_{50}$ values of compounds represent the concentration that caused 50% enzyme activity loss.

(**2**), platyphyllone (**3**), platyphyllonol-5-xylopyranoside (**4**), hirsutanonol (**5**), oregonin (**6**), rubranol (**7**), rubranoside B (**8**) and rubranoside A (**9**), respectively.[14,16)] Isolated compounds **1**–**9** were tested against SARS-CoV PL^{pro} using a continuous fluorometric assay. Of the isolated compounds (**1**–**9**), six
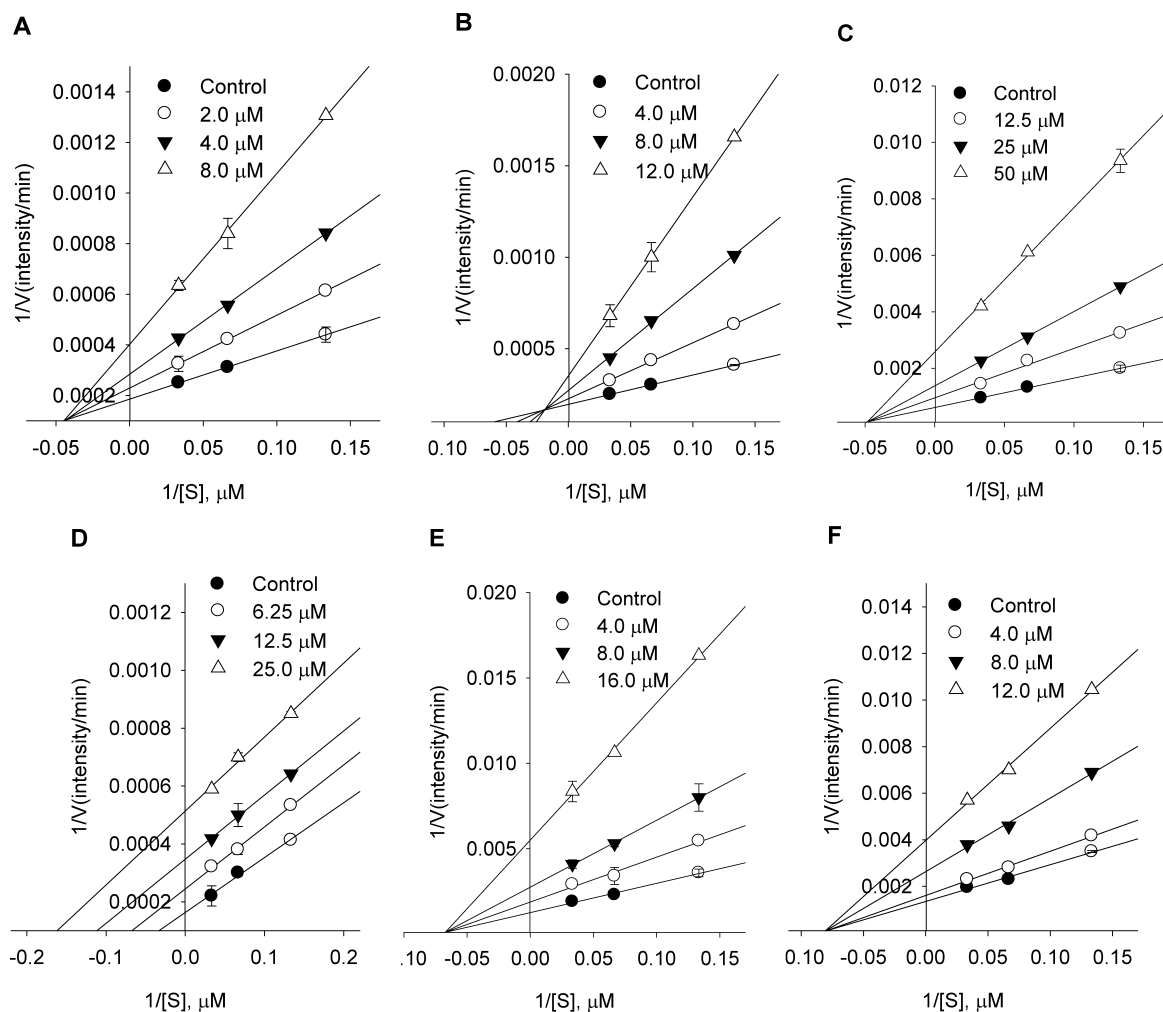
Fig. 4. Lineweaver–Burk Plots for the Inhibition of the Proteolysis of SARS-CoV PL^{pro} by Compounds [**2** (A), **5** (B), **6** (C), **7** (D), **8** (E), **9** (F), Respectively]

compounds (**2**, **5–9**) of isolated diarylheptanoids showed a dose-dependent inhibitory effect against the PL^{pro} (Fig. 3A). The diarylheptanoids were found to be reversible inhibitors because an increase in concentration rapidly reduced enzyme activity. Inhibitors with PL^{pro} inhibitory activity showed a similar relationship between enzyme activity and enzyme concentration [*e.g.*, see Fig. 3B for hirsutenone (**2**)]. The inhibitory activities of the first series of naturally derived diarylheptanoids against SARS-CoV PL^{pro} are reported in Table 1. The inhibitory activities are expressed as IC$_{50}$ values of the pure compounds **1–9**. The known viral protease inhibitor curcumin was used as a reference inhibitor (IC$_{50}$ value of 5.7 μM).

As shown in Table 1, the bioactivity of these compounds depended on the substituted groups in the diaryheptanoid scaffold. Of the tested diarylheptanoids **1–9**, compound **2**, containing an α,β-unsaturated carbonyl group with a catechol moiety in the backbone, was the most effective inhibitor, with an IC$_{50}$ value of 4.1 μM. Mono hydroxyl substitution on the terminal aromatic ring had a substantial effect on the inhibitory activity [compare, for example, **1** (IC$_{50}$ >200 μM), **2**]. All mono hydroxyl-substituted diarylheptanoids (**1**, **3**, **4**) are poorer inhibitors of PL^{pro} than the corresponding compounds (**2**, **5**, **6**) with the catechol moiety. When the three classes of diarylheptanoids (**2**, **5**, **7**) having an α,β-unsaturated carbonyl,

a β-hydroxyl carbonyl, and only a hydroxyl moiety in the C7 aliphatic molecule are compared, the α,β-unsaturated carbonyl moiety (**2**, IC$_{50}$=4.1 μM) proved to be 2-fold more effective than the other moieties (**5**, 7.8 μM, **7**, 12.3 μM, respectively). In the commonly adopted mechanism of inhibition of cysteine protease, a covalent bond is formed between the carbonyl group located at the warhead of the inhibitor and the active site cysteine residue in the enzyme. Improving the electronegativity at this warhead carbonyl moiety could accelerate the covalent bond formation. The α,β-unsaturated carbonyl is a good Michael acceptor and undergoes nucleophilic addition. Thus, the above finding suggests that the α,β-unsaturated carbonyl and catechol groups may play a pivotal role in SARS-CoV PL^{pro} inhibition by interacting with the PL^{pro} nucleophiles.

To determine the importance of the α,β-unsaturated carbonyl moiety in diarylheptanoid to the inhibition of SARS-CoV PL^{pro}, we synthesized the corresponding keto-enol derivatives (**10**, **11**) from curcumin, as shown in Chart 1.[24] As shown in Table 1, the demethylated curcumin **10**, with two α,β-unsaturated carbonyls in the molecule, exhibits potency comparable to those of the corresponding compound **2** and curcumin. However, the incorporation of a keto-enol into tetrahydrocurcumin afforded a less potent derivative (compound **11**,

$IC_{50}=59.8\,\mu M$).

When we compared diarylheptanoids with diarylheptanoid glycosides, we found that the activities of diarylheptanoids were higher than were those of their corresponding glycosides. Diarylheptnoids with glucopyranoside and xylopyranoside moieties, **4** ($IC_{50} >200\,\mu M$) and **6** ($IC_{50}=20.1\,\mu M$), respectively, had higher IC_{50} values than other diarylheptanoids (**1–3**, **5**). Bulky substituent like sugar moieties in the frame of the diarylheptanoid resulted in higher IC_{50} values. However, the substitution of the glycosides affecting the IC_{50} of the only hydroxyl group substituted in the C7 frame (**7–9**) cannot be ruled out. Compounds **8** and **9** exhibited modest activity, with IC_{50} of values 8.0 and 9.1 μM, similar to that of the corresponding inhibitor **7** ($IC_{50}=12.3\,\mu M$).

To determine if the isolated compounds described above might be inhibitor of SARS-CoV 3CL^{pro}, these compounds were tested using recombinant 3CL^{pro} expressed in our laboratory. As shown in Table 2, no detectable inhibition was observed at the tested concentration, indicating that diarylheptanoids have an interesting selectivity for the coronaviral proteases (PL^{pro} and 3CL^{pro}). Compound **2** ($IC_{50}=36.2\,\mu M$) also exhibited stronger 3CL^{pro} inhibition than the derivatives.

Furthermore, PL^{pro}, located within nsp3, cleaves at nsp1/2, nsp2/3 and nsp3/4 boundaries using the consensus motif LXGG, along with a consensus cleavage sequence of cellular deubiquitinating (DUB) enzymes.[8] It has become clear that deubiquitination may have important implications on viral replication and pathogenesis. To experimentally confirm the predicted DUB activity of the isolated diarylheptanoids (**1–9**), we observed the DUB activity for *in vitro* characterization. Table 2 lists the *in vitro* activity of compounds **1–9** against DUB. The IC_{50} values demonstrated that the presence of naphthalene in **2** ($IC_{50}=3.0\,\mu M$) and **8** ($IC_{50}=7.2\,\mu M$) provide a greater inhibitory effect than the other diarylheptanoid derivatives. In a similar vein, compounds **1**, **3**, and **4**, bearing mono hydroxyl substitution on the terminal aromatic ring, showed any inhibitory activity ($IC_{50} >200\,\mu M$). To date, there is no potent and selective chemical compound available for the inhibition of DUB. Thus, further investigation is necessary to determine the specifics of the inhibition with the diarylheptanoids and the PL^{pro}-DUB interaction

Finally, the kinetic behavior of SARS-CoV PL^{pro} at differing concentrations of compounds (**2**, **5–9**) was studied. Compounds **2**, **6**, **8**, and **9** displayed noncompetitive inhibition against SARS-CoV PL^{pro} as shown in Lineweaver–Burk plots (Figs. 4A, C, E, F) respectively (for instance all lines in the Lineweaver–Burk plot met at a nonzero point on the *x*-axis). On the other hand, compound **5** displayed different inhibition properties for SARS-CoV PL^{pro}. A similar analysis of these compounds shows a series of lines, which intersect to the left of the *y*-axis and above the *x*-axis (Fig. 2B), indicating that these inhibitors were mixed-type inhibitors. Interestingly, compound **7**, having only hydroxyl group substituted in the C7 frame, behaves as an uncompetitive inhibitor because both V_{max} and K_m values were affected by increasing concentrations of **7** (Fig. 4D).

In summary, we attempted to develop naturally derived SARS-CoV PL^{pro} inhibitors from *A. japonica*. We isolated nine diarylheptanoids **1–9** and evaluated their activity against PL^{pro} to study the structure-activity relationship and to select lead compound **2** with high potency against PL^{pro}. The above finding demonstrate that the catechol and α,β-unsaturated carbonyl moieties in diarylheptanoid are critical factors affecting SARS-CoV PL^{pro} inhibition activity. The IC_{50} value of this inhibitor, although higher than those of synthetic PL^{pro} inhibitors, is nonetheless in the low micromolar range. We believe that this lead structure will facilitate the design of more effective inhibitors against SARS-CoV infection.

REFERENCES

1) Berger A, Drosten Ch, Doerr HW, Stürmer M, Preiser W. Severe acute respiratory syndrome (SARS)—paradigm of an emerging viral infection. *J. Clin. Virol.*, **29**, 13–22 (2004).

2) Stadler K, Masignani V, Eickmann M, Becker S, Abrignani S, Klenk HD, Rappuoli R. SARS—beginning to understand a new virus. *Nat. Rev. Microbiol.*, **1**, 209–218 (2003).

3) Drosten C, Günther S, Preiser W, van der Werf S, Brodt HR, Becker S, Rabenau H, Panning M, Kolesnikova L, Fouchier RA, Berger A, Burguière AM, Cinatl J, Eickmann M, Escriou N, Grywna K, Kramme S, Manuguerra JC, Müller S, Rickerts V, Stürmer M, Vieth S, Klenk HD, Osterhaus AD, Schmitz H, Doerr HW. Identification of a novel coronavirus in patients with severe acute respiratory syndrome. *N. Engl. J. Med.*, **348**, 1967–1976 (2003).

4) Bartlam M, Yang H, Rao Z. Structural insights into SARS coronavirus proteins. *Curr. Opin. Struct. Biol.*, **15**, 664–672 (2005).

5) Yang H, Yang M, Ding Y, Liu Y, Lou Z, Zhou Z, Sun L, Mo L, Ye S, Pang H, Gao GF, Anand K, Bartlam M, Hilgenfeld R, Rao Z. The crystal structures of severe acute respiratory syndrome virus main protease and its complex with an inhibitor. *Proc. Natl. Acad. Sci. U.S.A.*, **100**, 13190–13195 (2003).

6) Anand K, Ziebuhr J, Wadhwani P, Mesters JR, Hilgenfeld R. Coronavirus main proteinase (3CLpro) structure: basis for design of anti-SARS drugs. *Science*, **300**, 1763–1767 (2003).

7) Han YS, Chang GG, Juo CG, Lee HJ, Yeh SH, Hsu JT, Chen X. Papain-like protease 2 (PLP2) from severe acute respiratory syndrome coronavirus (SARS-CoV): expression, purification, characterization, and inhibition. *Biochemistry*, **44**, 10349–10359 (2005).

8) Barretto N, Jukneliene D, Ratia K, Chen Z, Mesecar AD, Baker SC. The papain-like protease of severe acute respiratory syndrome coronavirus has deubiquitinating activity. *J. Virol.*, **79**, 15189–15198 (2005).

9) Wu CY, Jan JT, Ma SH, Kuo CJ, Juan HF, Cheng YS, Hsu HH, Huang HC, Wu D, Brik A, Liang FS, Liu RS, Fang JM, Chen ST, Liang PH, Wong CH. Small molecules targeting severe acute respiratory syndrome human coronavirus. *Proc. Natl. Acad. Sci. U.S.A.*, **101**, 10012–10017 (2004).

10) Shie JJ, Fang JM, Kuo TH, Kuo CJ, Liang PH, Huang HJ, Wu YT, Jan JT, Cheng YS, Wong CH. Inhibition of the severe acute respiratory syndrome 3CL protease by peptidomimetic α,β-unsaturated esters. *Bioorg. Med. Chem.*, **13**, 5240–5252 (2005).

11) Regnier T, Sarma D, Hidaka K, Bacha U, Freire E, Hayashi Y, Kiso Y. New developments for the design, synthesis and biological evaluation of potent SARS-CoV 3CL(pro) inhibitors. *Bioorg. Med. Chem. Lett.*, **19**, 2722–2727 (2009).

12) Ryu YB, Park SJ, Kim YM, Lee JY, Seo WD, Chang JS, Park KH, Rho MC, Lee WS. SARS-CoV 3CL^{pro} inhibitory effects of quinonemethide triterpenes from *Tripterygium regelii*. *Bioorg. Med. Chem. Lett.*, **20**, 1873–1876 (2010).

13) Ryu YB, Jeong HJ, Kim JH, Kim YM, Park JY, Kim D, Nguyen TT, Park SJ, Chang JS, Park KH, Rho MC, Lee WS. Biflavonoids

from *Torreya nucifera* displaying SARS-CoV 3CL^{pro} inhibition. *Bioorg. Med. Chem.*, **18**, 7940–7947 (2010).

14) Chou CY, Chien CH, Han YS, Prebanda MT, Hsieh HP, Turk B, Chang GG, Chen X. Thiopurine analogues inhibit papain-like protease of severe acute respiratory syndrome coronavirus. *Biochem. Pharmacol.*, **75**, 1601–1609 (2008).

15) Ghosh AK, Takayama J, Aubin Y, Ratia K, Chaudhuri R, Baez Y, Sleeman K, Coughlin M, Nichols DB, Mulhearn DC, Prabhakar BS, Baker SC, Johnson ME, Mesecar AD. Structure-based design, synthesis, and biological evaluation of a series of novel and reversible inhibitors for the severe acute respiratory syndrome-coronavirus papain-like protease. *J. Med. Chem.*, **52**, 5228–5240 (2009).

16) Lai YC, Chen CK, Lin WW, Lee SS. A comprehensive investigation of anti-inflammatory diarylheptanoids from the leaves of *Alnus formosana*. *Phytochemistry*, **73**, 84–94 (2012).

17) Lee WS, Kim JR, Im KR, Cho KH, Sok DE, Jeong TS. Antioxidant effects of diarylheptanoid derivatives from *Alnus japonica* on human LDL oxidation. *Planta Med.*, **71**, 295–299 (2005).

18) Tung NH, Kwon HJ, Kim JH, Ra JC, Ding Y, Kim JA, Kim YH. Anti-influenza diarylheptanoids from the bark of *Alnus japonica*. *Bioorg. Med. Chem. Lett.*, **20**, 1000–1003 (2010).

19) Sun H, Luo H, Yu C, Sun T, Chen J, Peng S, Qin J, Shen J, Yang Y, Xie Y, Chen K, Wang Y, Shen X, Jiang H. Molecular cloning, expression, purification, and mass spectrometric characterization of 3C-like protease of SARS coronavirus. *Protein Expr. Purif.*, **32**, 302–308 (2003).

20) Han YS, Chang GG, Juo CG, Lee HJ, Yeh SH, Hsu J, Chen TX. Papain-like protease 2 (PLP2) from severe acute respiratory syndrome coronavirus (SARS-CoV): expression, purification, characterization, and inhibition. *Biochemistry*, **44**, 10349–10359 (2005).

21) Grum-Tokars V, Ratia K, Begaye A, Baker SC, Mesecar AD. Evaluating the 3C-like protease activity of SARS-Coronavirus: recommendations for standardized assays for drug discovery. *Virus Res.*, **133**, 63–73 (2008).

22) Ratia K, Saikatendu KS, Santarsiero BD, Barretto N, Baker SC, Stevens RC, Mesecar AD. Severe acute respiratory syndrome coronavirus papain-like protease: structure of a viral deubiquitinating enzyme. *Proc. Natl. Acad. Sci. U.S.A.*, **103**, 5717–5722 (2006).

23) Li XQ, Andersson TB, Ahlström M, Weidolf L. Comparison of inhibitory effects of the proton pump-inhibiting drugs omeprazole, esomeprazole, lansoprazole, pantoprazole, and rabeprazole on human cytochrome P450 activities. *Drug Metab. Dispos.*, **32**, 821–827 (2004).

24) Venkateswarlu S, Ramachandra MS, Subbaraju GV. Synthesis and biological evaluation of polyhydroxycurcuminoids. *Bioorg. Med. Chem.*, **13**, 6374–6380 (2005).